Computers and Geotechnics 93 (2018) 123–132

Contents lists available at ScienceDirect

Computers and Geotechnics

journal homepage: www.elsevier.com/locate/compgeo

Research Paper

Numerical prediction and back-calculation of time-dependent behaviour of Ballina test embankment

Hans P. Jostad [a,*], Francesca Palmieri [a], Lars Andresen [a], Noel Boylan [b]

[a] NGI (Norwegian Geotechnical Institute), Sognsveien 72, 0855 Oslo, Norway
[b] NGI (Norwegian Geotechnical Institute), Level 7, 40 St. Georges Tce, Perth, WA 6000, Australia

ARTICLE INFO

Keywords:
Embankment
Soft soil
Consolidation
Settlements
Drains
FEM

ABSTRACT

The paper describes the Class A prediction and Class C back-calculations of the Ballina test embankment using the finite element program Plaxis and the Soft Soil Creep Model (SSCM). The prediction underestimated the measured settlement 3 years after construction by about 20%. This was mainly due to too high stiffness in the transition zone beneath the clay and that SSCM underestimated the shear deformation of the clay. Furthermore, the horizontal permeability of the clay was overestimated. In the back-calculation, it was possible to obtain a excellent match with the measured settlements by reasonable modifications of the input parameters.

1. Introduction

Settlements of foundations and embankments on soft ground in geotechnical engineering are often calculated using idealized 1D methods with simplified assumptions or elastic analytical solutions of load spread distribution with depths, pure vertical pore pressure dissipation, and permeability and compressibility parameters from oedometer tests. Time dependent creep deformations are added by a simple secondary consolidation term, e.g. Mesri [1]. However, in some projects more accurate settlement predictions are required. In these cases, 2D or 3D analyses using a fully coupled displacement and pore water flow (consolidation) finite element (FE) program with a proper material model may be used.

In order to improve the accuracy and reliability of more advanced numerical analyses, the FE calculation models and the process of determining parameters need to be validated against results from well defined and instrumented field cases. This was the purpose of the test embankments constructed at the National Soft Soil Testing Facility (NFTF) in northern New South Wales, Australia.

The Australian Research Council (ARC) Centre of Excellence for Geotechnical Science and Engineering invited practising engineers and academics to make predictions of the time dependent settlement, pore pressure dissipations and lateral displacements of the test embankment.

NGI delivered two different predictions, one based on hand-calculation and on based on advanced numerical analyses using the finite element program Plaxis (www.plaxis.nl). This paper describes the numerical Class A prediction together with a Class C back-calculation.

2. Background information

2.1. Test site and embankment

Two test embankments were constructed at the NFTF. Several sampling, laboratory and in situ testing campaigns have been performed to characterize the soil [2,3]. Based on geophysics, cone penetration (CPTU) and shear vane tests, it has been demonstrated that the stratigraphy is rather uniform across the site.

Seasonal groundwater variations of about ±1 m cause the in situ pore pressure to vary with time. The average ground water level is about 0.5 m below the ground. Data obtained from vibrating wire piezometers (VWP) installed within the Ballina clay below the footprint of the western embankment (i.e. the one with vertical drains) show that the groundwater is almost hydrostatic with depth.

The depositional history suggests that the ground is likely to be geologically normally consolidated as substantial erosion is unlikely to have occurred. However, some overconsolidation through the seasonal changes in groundwater levels and creep have occurred.

* Corresponding author.
E-mail address: hpj@ngi.no (H.P. Jostad).

http://dx.doi.org/10.1016/j.compgeo.2017.05.026
0266-352X/

The prediction is based on the stratigraphy deduced from CPT soundings and boreholes Inclo1, Mex1 and Inclo2, and aims at reproducing the settlement of the cross section 2 of the western embankment. The soil layering of this cross section comprises of about 1.4 m thick alluvial clayey sandy silt, underlain by a 9.4 m thick estuarine clay layer, a 3.3 m thick transition zone, a 5 m thick sand layer and then a stiff Pleistocene clay layer.

In order to build the embankment, a working platform approximately 95 m long by 25 m wide and 0.6 m thick was initially constructed. On top of this a 0.4 m thick sand layer was placed, before the wick drains were installed. Lastly, a 2 m thick top earth fill comprised of highly plastic clay was constructed on top of the sand layer. The final crest of the embankment was 80 m long by 16 m wide. The slope of the sides was 3:2 (H:V).

3. Finite element analyses

3.1. Finite element model

The numerical analyses are carried out by using the finite element (FE) program Plaxis 2D version 2016.01 (www.plaxis.nl). Fig. 1 shows the finite element model used in the Class A prediction. The model consists of 8 soil layers, the 0.6 m thick working platform, 0.4 m thick sand drain and the 2 m thick top embankment. The model covers a total horizontal distance of 140 m. This model is found to be sufficiently large enough such that end effects do not affect the settlement beneath the embankment and the horizontal displacement at the edge of the embankment. The bottom boundary is taken at the top of the stiff Pleistocene clay. The ground water table is in the Class A prediction taken at 1.2 m below the original terrain in order to fit the effective stress profile given in [2].

The effect of the wick drains is modelled by the vertical drain elements available in Plaxis, starting from the sand layer 1.0 m above the ground continuing down to 14.9 m below the ground, with a selected center distance of 3.2 m. When activated, the drains force the nodes with pore pressure degree of freedom along the geometrical line to have a head equal to a specified value. In the Class A prediction the head is set equal to 0 m, i.e. the nodes are forced to have a hydrostatic pore pressure starting from the original ground level. The corrected horizontal permeabilities used for the soil between the drains are calculated in Section 3.3.

The ground is assumed to be horizontal even though the borings shows some small variations. Displacements along the bottom of the model is fully fixed while the vertical boundaries are free to move in the vertical direction and fixed in the horizontal direction. Pore water flow is prevented through the bottom and the vertical boundaries of the estuarine layer. The other soil layers are considered to be drained and thus pore water flow through their vertical boundaries are allowed.

In the analyses an updated mesh formulation is used. This means that after each calculation step, the nodal points are moved according to the calculated incremental displacements. The main purpose of the updated mesh analyses is to account for that the excess weight of the embankment is gradually reduced as the material settle below the ground water table. This is accounted for by using the "Updated water pressures" option in Plaxis.

The 15-node triangular element and the medium mesh option are selected in the calculation, leading to a total of 2151 elements. This model is found to be fine enough to not be affected by any discretization errors.

3.2. Soil models and properties

The compressibility and shear deformation of the estuarine clay are modelled with the Soft Soil Creep Model (SSCM) [4]. This model accounts for the stress dependent stiffness of the soil within the framework of hardening plasticity. In addition, the model takes into account the time-dependent behaviour of the deformation, i.e. creep. The hardening law of SSCM does not include directly the strain-induced destructuration such as for instance in Creep-SCLAY1S [5,6]. Instead, the parameters are selected in order to model the significant stiffness reduction seen for this clay beyond the yield (pre-consolidation) stress in the stress range of interest. Thus, a strain independent value of the modified compression index λ^* is assumed to be appropriate to describe the material compressibility. The SSCM uses an associated plastic flow rule based on an isotropic CamClay type cap surface as shown in Fig. 2 (left). The hardening law is controlled only by the plastic volumetric strain. This means that the additional shear deformation due to slightly higher shear mobilisation than the K_o^{NC} -state may be different than predicted by the isotropic SSCM model. However, in order to control the shear deformation one need to include one additional parameter that change the shape of the yield surface between the K_o^{NC} -line and the failure line M. In the paper by Sivasithamparam et al. [7], one such model is proposed.

The input parameters to the SSCM that controls the compressibility are the modified compression index, λ^*, the modified swelling index, κ^*, the unloading/reloading Poisson ratio, ν_{ur}, the modified secondary compression index, μ^*, and the vertical effective yield stress, σ_{vc}'. The yield stress is defined by the over-consolidation ratio, $OCR = \sigma_{vc}'/\sigma_{vo}'$, or pre-overburden pressure, $POP = \sigma_{vc}' - \sigma_{vo}'$. In SSCM, it is assumed that all plastic strain is time dependent. This means that the yield stress given by the intersection between the elastic compression line and the elasto-plastic virgin compression line is rate dependent, see Fig. 2 (right). The creep rate along the virgin compression line is $d\varepsilon/dt = \mu^*/t_{eqv}$, where t_{eqv} is given by a vertical strain increment (distance) from a reference line corresponding to $t_o = 24$ h, i.e. $\Delta\varepsilon_{v,creep} = \mu^* \ln(t_{eqv}/t_o)$. Therefore, when interpreting the input parameters to SSCM from a constant rate of strain (CRS) oedometer test, one need to account for the actual strain rate used in the CRS-test. Fig. 3 shows back-calculation of the CRS-test of the specimen from depth 5.49 m in boring Inclo2 using SSCM with $\lambda^* = 0.263$, $\kappa^* = 0.042$, $\mu^*/\lambda^* = 0.03$, $\sigma_{vo}' = 40.5$ kPa and $\sigma_{vc}' = 64$ kPa (at the reference

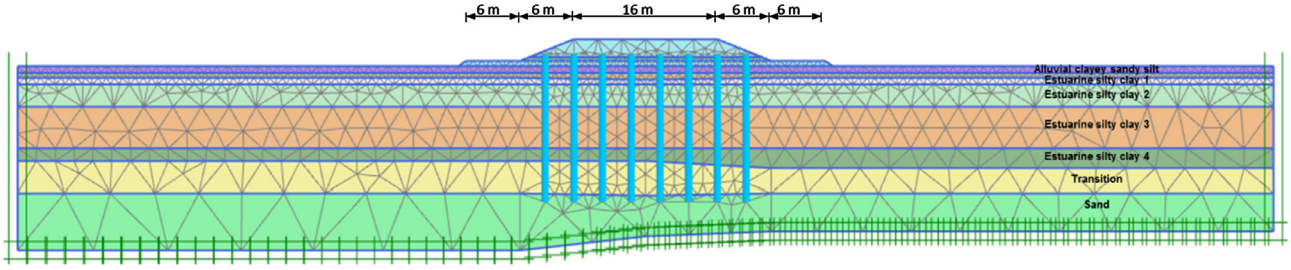

Fig. 1. Finite Element Model of cross section 2 used in the Class A prediction.

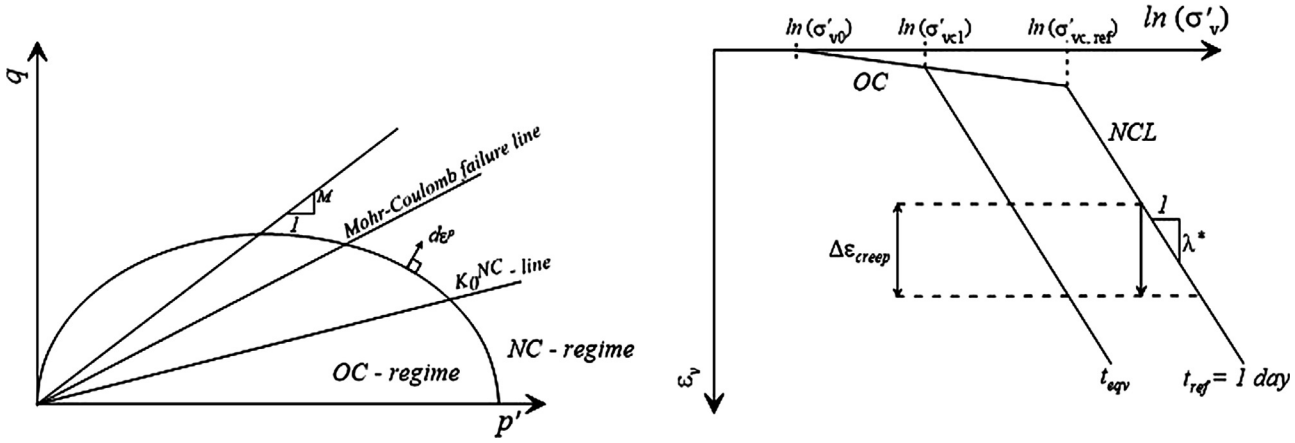

Fig. 2. The Soft Soil Creep Model, yield surface (left) and compression curves (right).

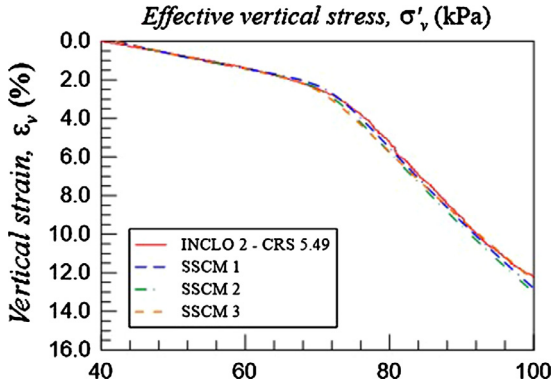

Fig. 3. Back-calculation of CRS test INCLO2_5.49m using the Soft Soil Creep Model with three different sets of input parameters.

strain rate of 1 day) or a *POP* of 23.5 kPa, applying a strain rate of $d\varepsilon/dt$ = 28%/day. This is called material set SSCM1 in Fig. 3. This automatically accounts for the rate dependent yield stress found in the CRS-tests. However, a good fit to the CRS-curve could also be obtained by increasing the creep ratio μ^*/λ^* from 0.03 to 0.04 and increasing σ_{vc}' from 64 to 66 kPa (SSCM2), or reducing λ^* from 0.263 to 0.24 and decreasing σ_{vc}' from 66 to 62 kPa (SSCM3). In the calculation of the settlement of the embankment, the effect of changing μ^*/λ^* has largest effect since it increases the contribution from creep when extrapolating from the CRS strain rate to the significantly slower strain rate in the field. In addition, the creep rate as function of OCR is governed by the exponent, $n = \mu^*/(\lambda^*\text{-}\kappa^*)$, which affect the creep rate to the side of the embankment not experiences increased effective stresses. The same type of back-calculation is performed for the other CRS-tests on specimens from Inclo2. Since the simulations of the CRS-tests start at a low isotropic effective stress, the results are also dependent on v_{ur}, which controls the effective stress ratio, $\Delta\sigma_h'/\Delta\sigma_v' = v_{ur}/(1\text{-}v_{ur})$, before yielding and the effective stress ratio $K_o^{NC} = \sigma_h'/\sigma_v'$ at the vertical yield stress σ_{vc}'. The Poisson's ratio, v_{ur}, is assumed for all layers equal to 0.2. In particular, for soft clays it represents an average value, while this value represents a lower limit for silty sand and sand as shown by Das [8]. The initial lateral earth pressure coefficients K_o are defined according to Pineda et al. [2].

Based on Fig. 12b in [2], a constant $\mu^*/\lambda^* = C_\alpha/C_c = 0.03$ was used for the estuarine soft clay in the Class A prediction.

The back-calculated input parameters from the CRS tests are shown in Fig. 4. The estuarine soft clay is divided into 4 layers, with constant properties within each sub-layer. The parameters are therefore average values within each sublayer.

The Soft Soil Model (SSM) is applied for the alluvial clayey sandy silt between 0.75 and 1.4 m depth and for the transition zone (10.8–14.0 m). SSM is similar to SSCM, however, without the effect of time dependent creep. For the alluvial soil and transition zone, compressibility parameters are defined based on the available oedometer tests. For the alluvial silt, there is only one oedometer test at a depth of 0.79 m from Inclo2. From this test it is seen that the yield stress is more diffuse and that the stiffness at large stresses is higher than for the clay. The best fit of κ^*, λ^* and *POP* for the actual stress range to this material is also given in Table 1. Since the stress-dependent stiffness in SSM may lead to unrealistic deformations in the most superficial part of the deposit, the upper 0.75 m of the alluvial soil is modelled assuming a constant oedometer modulus E_{oed} = 6900 kPa, adopting the Mohr-Coulomb model. This value is uncertain and can be both higher and lower, however the contribution to the total settlement is in any cases rather small.

A similar approach is used for the transition zone. The oedometer test (sample from depth 11.46 m) shows no clear yield stress within the stress range considered, i.e. up to a stress of about 700 kPa. However, the observed nonlinear behaviour is fitted by a "bi-linear" curve with λ^* = 0.015 and κ^* = 0.009, and *POP* = 21 kPa. Due to the significantly stiffer response of this material, the depth where this zone is included affects the calculated settlement.

The Hardening Soil Model (HSM) is used for the sand layer below the transition zone. Compressibility parameters are for the sand layer defined by empirical correlations in Lunne et al. [9], based on the measured cone resistance, q_t. The main properties used in the analyses are the reference Young's modulus at 50% shear mobilisation, E_{50}^{ref} = 66 MPa, oedometer modulus, E_{oed}^{ref} = 82 - MPa, unloading/reloading Young's modulus, E_{ur}^{ref} = 161 MPa, a reference stress, p_{ref} = 100 kPa, moduli exponent, m = 0.5 and friction angle, ϕ = 42.5°. However, the contribution from this layer to the total settlement is found to be negligible.

The vertical consolidation coefficient, c_v is assumed based on Pineda et al. [2]. In addition, these values are modified for taking into account the smear effects due to the installation of prefabricated vertical drains and the influence of modelling a radial flow pattern of drainage with a 2D model as described in Section 3.3.

The most relevant parameters for the clay and silt layers used in the prediction are listed in Table 1.

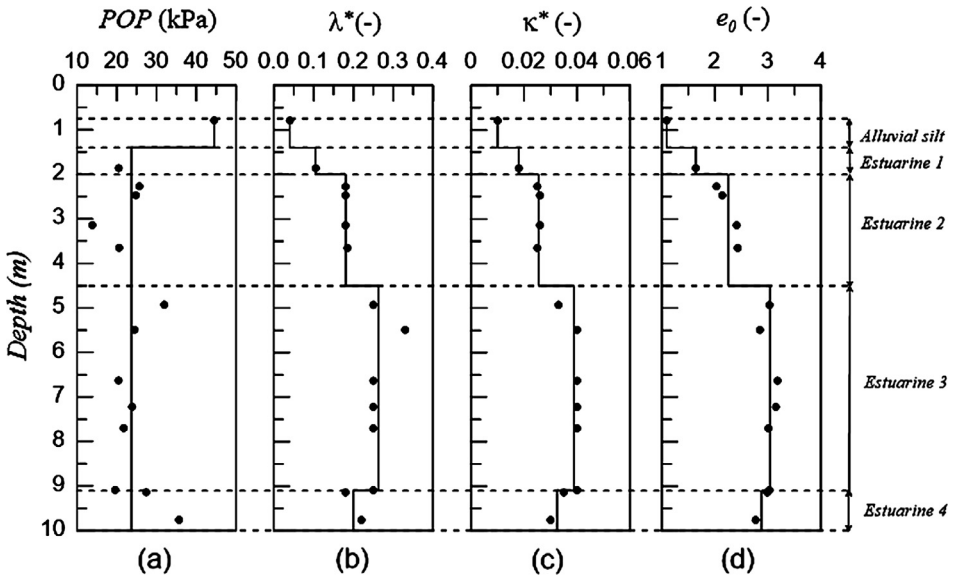

Fig. 4. Input parameters used in back-calculation of CRS tests on samples from Inclo2 using the Soft Soil Creep Model and values (given by the vertical solid lines) used in the class A prediction.

Table 1
SSCM/SSM input parameters for the clay/silt layers used in the Class A prediction.

Layer	Depth [m]	γ [kN/m^3]	λ^* [–]	κ^* [–]	μ^*/λ^* [–]	K_o^{NC} [–]	k_v [m/day]	k_h [m/day]	*POP* [kPa]	$K_o^{initial}$ [–]
Alluvial silt	0.75–1.4	17.3	0.04	0.01	–	0.47	6.4e−3	16.0e−3	44.5	0.90
Estuarine 1	1.4–2	14.4	0.10	0.018	0.03	0.4	0.4E−3	1.0E−3	24	0.55
Estuarine 2	2–4.5	14.4	0.181	0.026	0.03	0.4	0.4E−3	1.0E−3	24	0.55
Estuarine 3	4.5–9.1	14.4	0.263	0.039	0.03	0.4	0.4E−3	1.0E−3	24	0.55
Estuarine 4	9.1–10.8	14.4	0.20	0.033	0.03	0.4	0.4E−3	1.0E−3	24	0.55
Transition zone	10.8–14.0	19.1	0.016	0.009	–	0.38	0.5e−3	1.3e−3	21	0.55

3.3. Wick drains

Preinstalled vertical drains (PVDs) installed at a square grid spacing of 1.2 m cover the 24 m width of the main embankment area. The PVDs are assumed to be draining at the sand layer above the working platform and at the base level at 14.9 m depth below the ground where they are penetrated into the sand layer. The consolidation of the estuarine clay layer beneath the embankment is therefore assumed to be dominated by horizontal drainage towards the PVDs. The vertical drains have thus been modelled considering a system of unit cells as shown in Fig. 5 with each drain at the centre of a unit cell with equivalent diameter $d_e = 1.05 \times 1200$ mm = 1260 mm.

The equivalent diameter of the wick drain was calculated as $d_w = 2\cdot(w + t)/\pi = 2 \cdot (100\text{ mm} + 3\text{ mm})/\pi = 66$ mm. The dimensions (t and w) are taken from the specifications of the CeTeau drain. The drains were installed using a rectangular shaped mandrel with dimensions 120 mm × 60 mm giving an equivalent diameter of the mandrel $d_m = 115$ mm. It is assumed a smeared (remoulded) zone of diameter d_s and reduced permeability k_s around each drain caused by installation. Based on recommendations in Hansbo [9] $d_s = 2.0 \cdot d_m = 230$ mm and the reduced permeability k_s is assumed as $k_s = k_h/3$.

The average degree of drainage U within each cell of PVDs is calculated for each layer based on Hansbo [9] accounting for installation smear effects but neglecting any flow resistance of the drains:

$$U(t) = 1 - \exp\left(\frac{-8T_r}{F_n}\right) \quad (1)$$

$$T_r = \frac{C_h \cdot t}{(d_e)^2}$$

$$F_n = \frac{n^2}{n^2 - 1} \cdot \left(\ln\left(\frac{n}{s}\right) + \left(\frac{k_h}{k_s}\right)\ln(s) - 0,75\right)$$

where c_h is the horizontal coefficient of consolidation, t is the consolidation time, $n = d_e/d_w$ and $s = d_s/d_w$. With this approach the average degree of consolidation $U(t)$ at any consolidation time can be calculated. It is noted that this approach assumes at any time a constant degree of drainage and thus a constant value of excess pore pressures within the entire zone of PVDs for a given soil layer.

In the 2D model, the same time to 90% degree of drainage, t_{90} is obtained by using $B = 3.2$ m as the distance between the vertical drains and an equivalent horizontal permeability k_{ekv} equal to the intact horizontal permeability k_h.

In the Class A prediction, it was assumed a vertical coefficient of consolidation at the vertical yield stress of about 2 m^2/year. Based on experience from Sweden [10], the horizontal permeability was taken as 2.5 times the vertical permeability. The calculated time for 90% degree of drainage was approximately 0.4 year = 150 days.

In Fig. 10a in [2], it is shown that c_v may be even smaller than 1 m^2/yr at an effective vertical stress between 100 and 200 kPa. The lowest value is about 0.3 m^2/yr at a depth of 7.70 and 9.73 m. With $c_h = c_v = 0.3$ m^2/yr, the time to reach 90% degree of drainage increases to about 9 years, demonstrating the large uncertainties in the predicted drainage time.

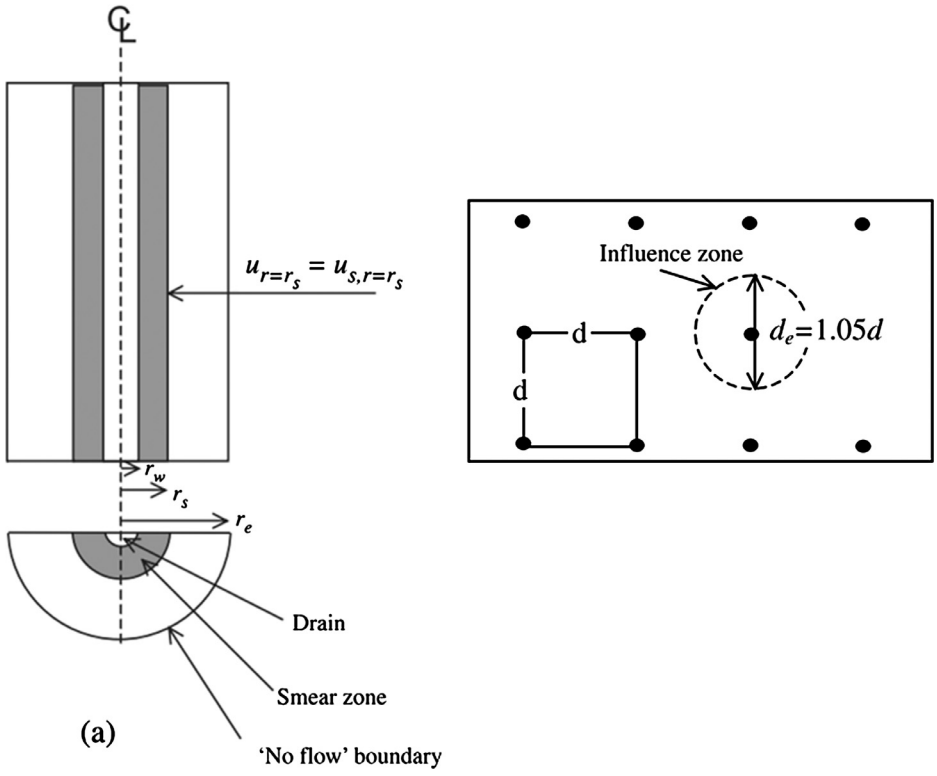

Fig. 5. Representation of system of PDVs by the unit cell approach.

3.4. Calculation phases

For cross section 2, settlement recording starts before the working platform construction. An initial consolidation phase of 8 days is considered leading to have comparable results. Drains are activated in four different phases, thus, taking into account the installation time of the vertical drains. The equivalent permeabilities were introduced when half of the drains were installed. Information about the calculation phases are listed in Table 2.

In the consolidation phases the automatic time stepping procedure in Plaxis was used. That the applied time steps were not too large was manually checked by inspection of the calculated history curves.

Table 2
Construction phases applied in the numerical analyses.

Phase	Time
Initial phase	–
Consolidation	8 days
Working platform construction	5 days
Consolidation	7 days
Drainage sand construction	8 days
Consolidation	8 days
Activate drains 1	1 day
Activate drains 2	1 day
Consolidation with eqv. permeabilities	5 days
Activate drains 3	1 day
Activate drains 4	1 day
Consolidation	5 days
Main construction	13 days
End of consolidation and creep	1770 days

3.5. Class A prediction and comparison with measurements

The calculated settlement of the original terrain at the center of cross section 2 versus time is compared with the measured settlements in Fig. 6. The most representative settlement plates are SP2 and SP3. However, as shown in Fig. 6, there are very small differences between the four settlement plates. The calculated settlement agrees very well with the measured settlement up to the end of filling. After that, the calculation first overestimates the rate of settlement, before both the rate and total settlement become too small. In July 2016, the calculated settlement is about 1.18 m while the measured settlements are between 1.46 and 1.52 m. The corresponding rate of calculated and measured settlement in July 2016

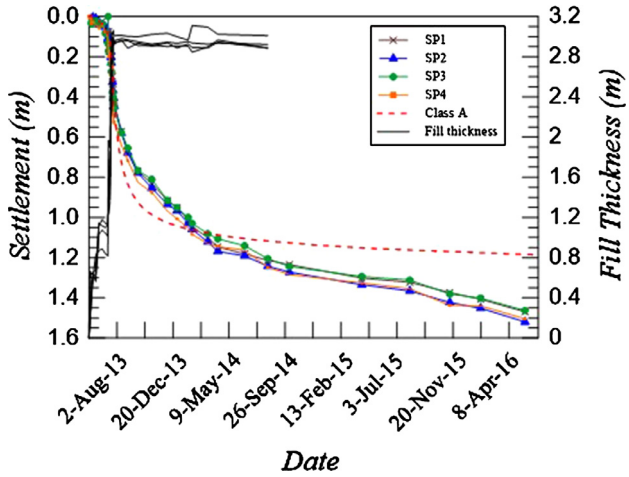

Fig. 6. Comparison between measured and calculated (Class A) time settlements curves.

is about 40 mm/year and 1000 mm/year. The main reason for the larger calculated settlement rate immediately after the construction of the fill is due to overestimation of the rate of pore pressure dissipation as will be shown later, while the most likely reason for under-predicting the settlement and rate of settlement in July 2016 will be discussed in the following.

Fig. 7 shows the calculated and measured settlement profiles at Mex1 in July 2016. From this figure, it is seen that one reason for the under predicted settlement is that the calculated compaction of the transition zone at 10.8–14 m depth is too small. At 11 m depth the measured settlement is about 6 cm larger than calculated. In addition, between 2 and 5 m depth the measured compaction is about 14 cm larger than calculated. Finally, in the top 2 m of the soil profile the measured compaction is about 13 cm while the calculated compaction is about 6 cm smaller.

Fig. 8 shows the calculated and measured average vertical strain in Mex1. This shows the same results as in Fig. 7, that the largest contributions to the under prediction come from the upper part of the estuarine clay, and beneath and above the estuarine clay.

Fig. 9 shows the calculated and measured horizontal displacement profiles with depth in Inclo1 at the end of construction and in July 2016. The calculated and measured horizontal displacement at the end of construction agree rather well, although, the measured displacements is larger below 8 m. The measured maximum horizontal displacement in July 2016 is 22 cm, while the calculated is only 10 cm. This means that the model was not able to predict the development of horizontal displacement with time, which more or less follows the development of settlement with time. This additional shear deformation is therefore one reason for the under estimated settlement between 2 and 5 m depth.

Fig. 10 shows the calculated and measured total pore pressure at 2, 6 and 10 m depths. The calculated pore pressures are initially too small and also decreases faster with time compared with the measured values. The calculation automatically accounts for the effect of piezometers (nodes) being moved downwards with the settlement. As the position of the ground water table is assumed to be fixed, the hydrostatic pore pressure is then increased due to the increased depth below the ground water table.

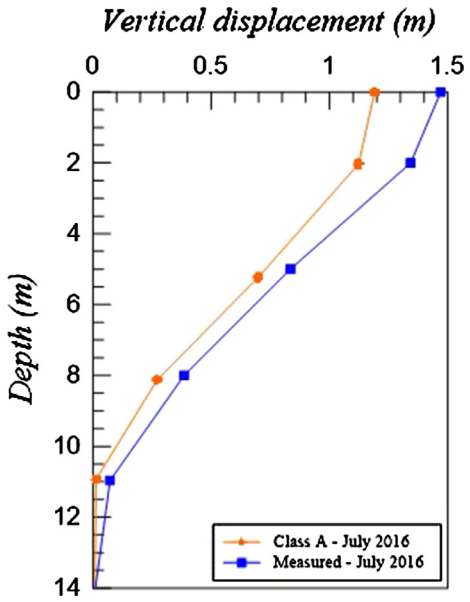

Fig. 7. Comparison between measured and calculated (Class A) settlements profiles in July 2016 at Mex1.

3.6. Uncertainties in Class A prediction

The following main uncertainties affected the predicted time-settlement curve:

- The measured permeability is varying significantly within the estuarine clay (from $6{\cdot}10^{-10}$ m/s at 9.73 m depth to $6{\cdot}10^{-8}$ m/s at 3.65 m depth, both at the yield stress, based on Table 2 in Pineda et al. [2]. In addition, based on experiences from Sweden [10], the intact horizontal permeability was taken as 2.5 times the vertical. However, the permeability anisotropy might be different for the estuarine clay.
- Limited information was available about the stiffness of the soil above and below the estuarine clay, i.e. only CRS-tests at 0.79 and 11.46 m in Inclo2.
- The ground water table is varying with the seasons and it may increase up to the sand drainage layer during the consolidation process.
- Spatial variation in the soil properties and layer thicknesses. The soil properties were based on CRS-tests on samples taken from Inclo2.
- The effect of the disturbance of the soil during installation of the drains. The permeability k_s in the remoulded (smear) zone around the drains was assumed to have a horizontal permeability being 1/3 of the intact horizontal permeability. However, this permeability can be both higher and lower.
- The stress path in the CRS-tests before yielding is different from in situ since it starts from significantly lower effective stresses in the CRS-tests. This may affect the predicted yield stress.
- SSCM may predict wrong shear strains for a shear mobilisation larger than the K_o^{NC}-line.
- The creep parameter is uncertain, $\mu^*/\lambda^* = C_\alpha/C_\alpha$ is varying between 0.025 and 0.07 in the IL creep tests presented in Pineda et al. [2].
- The idealization of the varying properties with depth within the estuarine soft clay into four sub-layers introduce some uncertainties.

A systematic evaluation of the uncertainties in the calculated settlement is presented in a companion paper by Liu et al. [11].

4. Class C back-calculation

4.1. Required modifications

Based on comparison between predicted and measured results, the following modifications are included in the Class C back-calculation:

- Based on the measured pore pressure before construction, the ground water level was increased from 1.2 m to 0.9 m below the ground surface. In order to keep the same vertical yield stress, POP was correspondingly increased by 3 kPa.
- The depth to the top of the transition zone is increased from 10.8 m to 11.0 m. Furthermore, in order to account for the gradual increase in sand content and thus increase in stiffness, a lower stiffness is given to the top 1 m of this layer using the Soft Soil Creep Model. By including the creep the POP needed also to be changed.
- The stiffness of the alluvial soil is reduced.
- The equivalent permeabilities of the estuarine clay are reduced. This is justified by the significantly lower c_v found in Fig. 10a in [2] compared to the values at the yield stress in Table 2 in the same paper. Furthermore, there are limited justifications for using a higher horizontal permeability than the vertical.

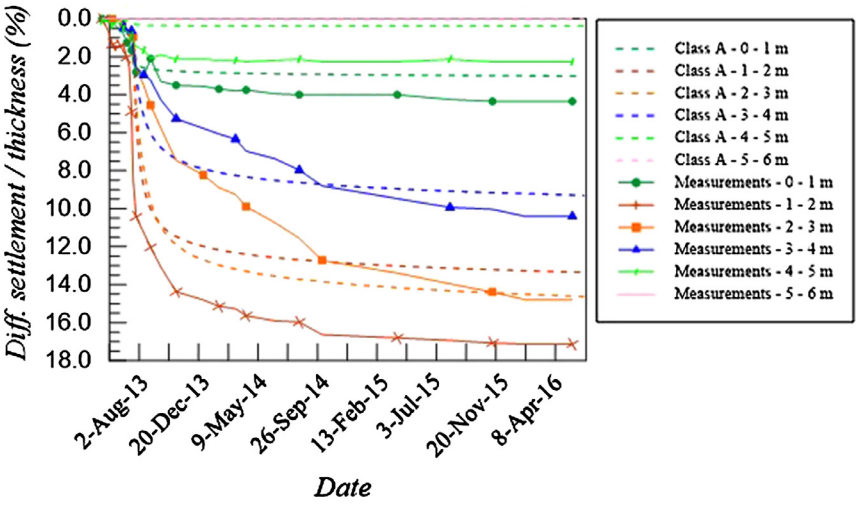

Fig. 8. Comparison between measured and calculated (Class A) average strain curves at Mex1.

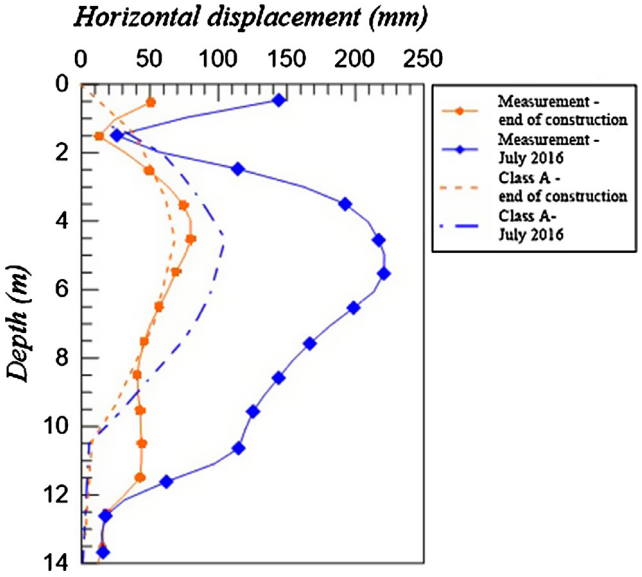

Fig. 9. Comparison between measured and calculated (Class A) horizontal displacement profiles in Inclo1in July 2016.

Instead, the small differences between the measured c_h and c_v as well as k_h and k_v suggest a low permeability anisotropy for the estuarine clay (Kelly et al. [3])

- The stiffness of the top estuarine clay between 2.0 and 4.5 m is reduced. This is partly done in order to compensate for that the SSCM underestimates the shear deformation.
- The creep index is increased to $\mu^*/\lambda^* = 0.05$ for the estuarine clay between 4.5 and 11 m.
- In order to increase the shear deformation and corresponding horizontal displacements at the periphery of the embankment, the K_o^{NC} is increased (i.e. the M-value defining the cap-surface, shown in Fig. 3 (left), is reduced). In some cases it was even necessary to reduce the friction angle, since the M-value cannot be less than the corresponding Mohr Coulomb failure line, $M = 6\sin\phi/(3-\sin\phi)$ in triaxial compression.

4.2. Modified soil properties

The stiffness of the Alluvial soil and the Transition zone were first reduced in order to fit the measured settlement profile after 3 years shown in Fig. 7, i.e. the average vertical strain in these zones. Then, the K_o^{NC} was increased in the Estuarine clay layers in order to increase the shear deformations in the soil beneath the

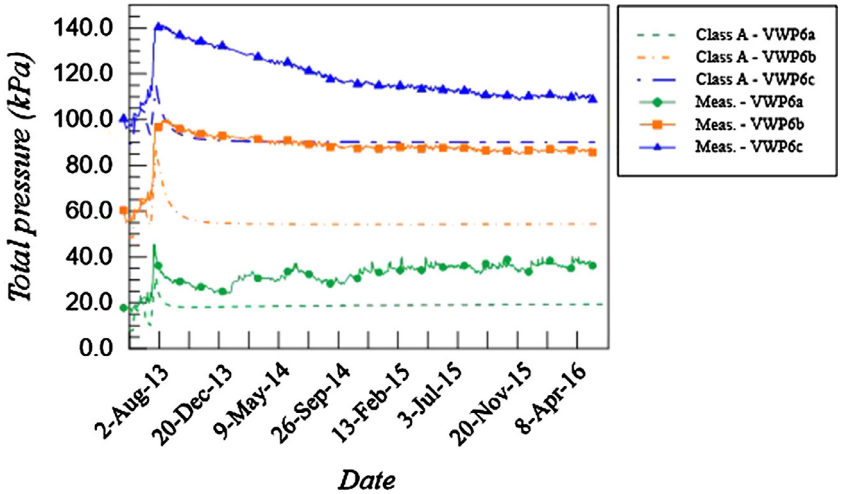

Fig. 10. Comparison between measured and calculated (Class A) total pore pressure histories in VWP6.

embankment and thus better fit the measured horizontal displacement profile at the edge of the embankment shown in Fig. 9. Finally, the SSCM input parameters λ^*, μ^*/λ^* and k_{ekv} were adjusted until a good fit with the measured average vertical strain curves, shown in Fig. 8, were obtained. It was chosen to keep the vertical yield stresses the same as for the Class A prediction. The adjustments were performed by first changing k_{ekv}, to fit the initial part of the strain curves (e.g. typically the first 6 to 12 months). The λ^*-values were then adjusted in order to fit the magnitude of the measured average strains after 3 years. Finally, the slope of the measured average vertical strain curves in July 2016 were fitted by changing the contribution from the creep, i.e. the μ^*/λ^*-ratios. This process was repeated until a good fit was obtained. The effect of changing the different parameters is demonstrated in Fig. 11. The figure shows the effect of increasing the equivalent permeability k_{ekv} by 50%, λ^* by 20% and μ^* by 20% compared to the parameters that gave the best fit to the average vertical strain between Magnets 2 and 3. The final parameters used in the Class C prediction are presented in Table 3.

By simulating CRS tests, however by starting from the initial effective stresses, it is demonstrated that the modified parameters given in Table 3 still agree with the CRS-tests from Inclo2 as shown Fig. 12.

4.3. Comparison with measurements

Fig. 13 shows that the Class C back-calculation gives time-settlement curves that perfectly fits the measured settlement curves at Mex1. From Fig. 6, it is seen that in order to improve the results compared to the Class A prediction, the total settlement

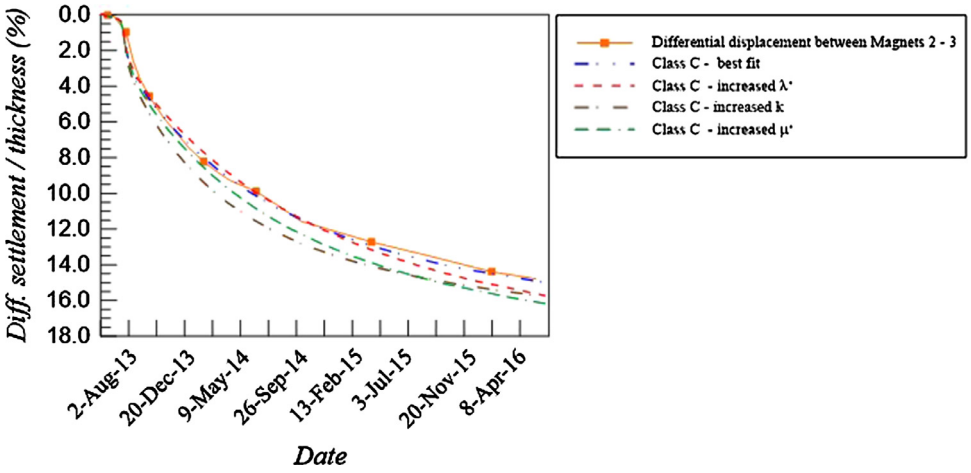

Fig. 11. Effect of changing the SSCM input parameters compared to the best fit parameters for the average vertical strain between Magnets 2 and 3.

Table 3
SSCM/SSC input parameters for the clay/silt layers in the Class C back-calculations.

Layer	Depth [m]	γ [kN/m^3]	λ^* [–]	κ^* [–]	μ^*/λ^* [–]	K_o^{NC} [–]	k_v [m/day]	$k_{vekv,\ h}$ [m/day]	*POP* [kPa]	K_o^{intial} [–]
Alluvial 2	0.75–1.5	17.3	0.05	0.010	–	0.73	0.01	0.01	47.5	0.58
Estuarine 1	1.5–2.0	14.4	0.15	0.018	0.04	0.73	1.50E−3	1.50E−3	27	0.58
Estuarine 2	2.0–4.5	14.4	0.20	0.020	0.04	1.94	0.80E−3	0.80E−3	27	0.62
Estuarine 3	4.5–9.1	14.4	0.24	0.039	0.05	0.73	0.08E−3	0.04E−3	27	0.58
Estuarine 4	9.1–11.0	14.4	0.18	0.033	0.05	0.73	0.05E−3	0.02E−3	27	0.58
Transition 1	11.0–12.0	19.1	0.08	0.015	0.04	0.73	0.32E−3	0.32E−3	27	0.58
Transition 2	12–14.25	19.1	0.03	0.010	0.03	0.73	0.60E−3	0.60E−3	50	0.58

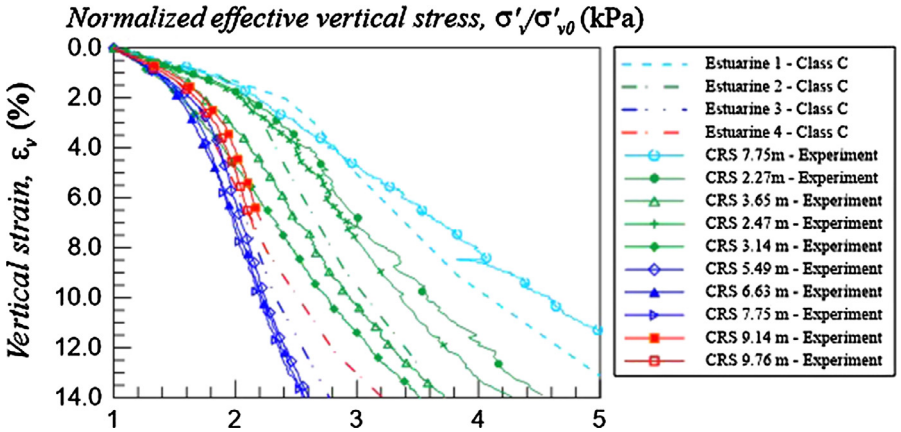

Fig. 12. Simulated CRS tests at characteristic depths within each of the Estuarine clay layers using modified parameters for the Class C calculation together with some CRS tests from Inclo2.

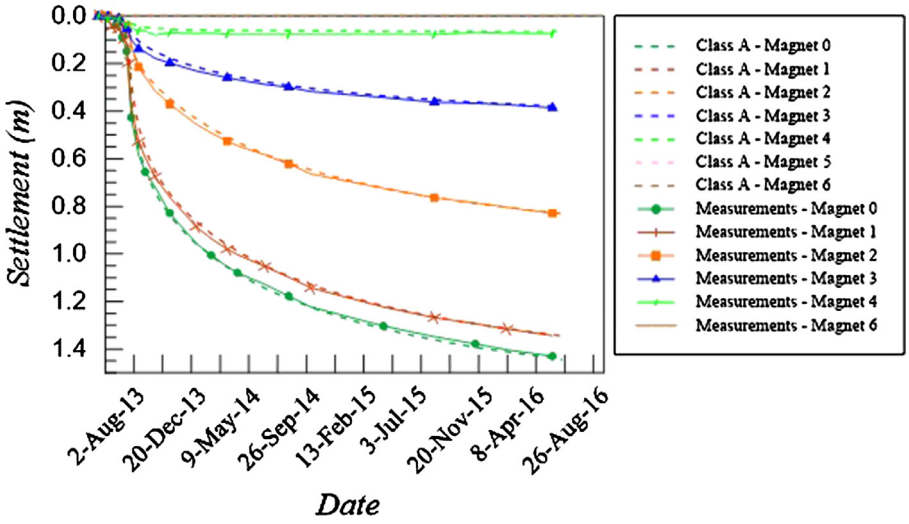

Fig. 13. Comparison between measured and calculated (Class C) time settlements curves.

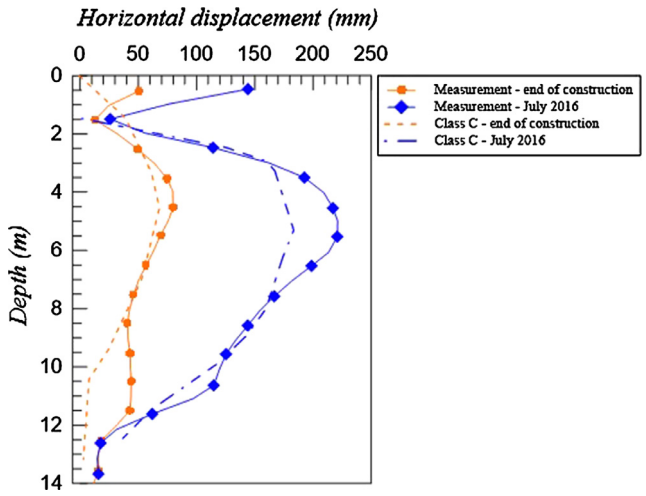

Fig. 14. Comparison between measured and calculated (Class C) horizontal displacement profiles in Inclo1.

after 3 years needed to be increased, and the rate of settlement needed to initially be reduced and after about 1 year to be increased. Based on Fig. 8, it is seen that the strain in the upper part of the estuarine clay (between 1 and 2 m depths) first of all needed to be increased. From Tables 1 and 3, it is seen that λ^* was increased from 0.1 to 0.15. This correction could be justified by too few tests within the actual depths and correspondingly large uncertainty in the actual parameter. In addition, it was necessary to compensate for that the material model, SSM, is underestimating the shear deformation in this layer. The increased settlement rate after 1 year, is obtained by a reasonable increase in the creep contribution, i.e. μ^*/λ^*-is increased from 0.03 to 0.04 in the upper part of the estuarine clay and 0.05 between 4.5 and 11 m. This means that the creep strain after 3 years may be as large as $\varepsilon_{creep} = -\mu^* \ln(t/t_{ref}) = 0.05 \cdot 0.2 \cdot \ln(3 \cdot 365 \text{ days}/1 \text{ day}) = 7\%$. This means that the contribution due to creep for this clay is significant. In addition, the equivalent permeability between 4.5 and 11 m depths is reduced from 1E−3 m/day to 0.02–0.04E−3 m/day. The parameters used in the Class C prediction can still be justified by the values in [2].

Fig. 14 shows that the horizontal displacement in July 2016 is also increased at the periphery of the embankment and agrees significantly better with the measurements at Inclo1 compared to the

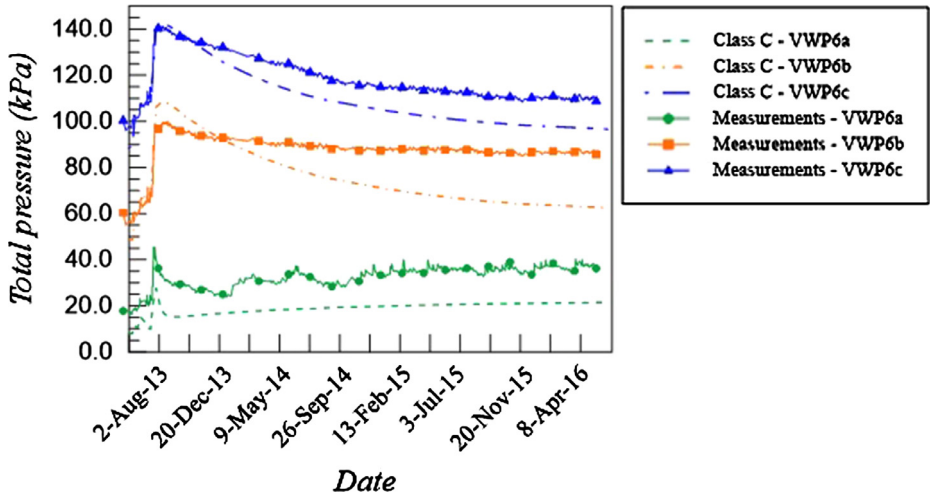

Fig. 15. Comparison between measured and calculated (Class C) total pore pressure histories in VWP6.

Class A prediction. In order to obtained better results another material model than the SSC model is recommended to be used as discussed in Section 3.2.

Fig. 15 shows that the calculated pore pressure histories also fits the measured histories better. The main reason for this is the lower equivalent permeablies used, as discussed above. Furthermore, the plane-strain idealization of the drains may overestimate the pore pressure dissipation in the middle between the drains.

5. Conclusions

The paper describes the Class A prediction and Class C back-calculations of the test embankment at the NFTF near Ballina in Australia using the FE program Plaxis 2D. The Soft Soil Creep Model (SSCM) was used for the deformation calculation of the soft estuarine clay. The Class A prediction underestimated the measured settlement 3 years after construction by about 20%. This was due to uncertainties in the creep index of the soft estuarine clay and the stiffness of the soil above and below the soft clay. SSCM was also underestimating the shear deformation of the soft estuarine clay. In addition, the horizontal permeability was overestimated based on wrong assumptions regarding the anisotropy ratio and neglecting the effect of reduction due to void ratio decrease below the yield stress. This effect could have been accounted for by using a void dependent permeability formulation available in Plaxis. However, since equivalent horizontal permeabilities are used that account for remoulding during installation of the drains and the idealization of the 3D flow pattern by a 2D model, made it difficult to use this feature. But, it is checked that the uncorrected vertical permeabilities used in the analysis agree with the void ratio dependent permeabilities in Fig. 11a in Pineda et al. [2].

In the Class C back-calculation, it was possible to obtain perfect match with the measured settlements by reasonable modifications of the input parameters. SSCM is thus generally well suited for modelling settlements of embankments on soft clay including the important contribution from creep. However, SSCM may underestimate the shear deformations for shear stress ratios above the K_o^{NC}-line. This can be mitigated by lowering the top point of the Cam-Clay cap surface given by M (i.e. increasing K_o^{NC}) and reducing the friction angle below the measured value from the triaxial tests. Alternatively, a model [7] that accounts for this effect by an input parameter that control the curvature of the yield surface could be used.

Acknowledgements

The authors gratefully acknowledge the support through an internal research project (GBV) which is partially funded by the Norwegian Research Council. In addition fruitful discussions with the authors (Suzanne Lacasse, Zhongqiang Liu and Jung Chan Choi) of the companion paper regarding uncertainties in the calculated results.

This research did not receive any specific grant from funding agencies in the public, commercial, or not-for-profit sectors.

References

[1] Mesri G. Coefficient of secondary compression. J Soil Mech Found Div ASCE 1973;99(1):123–37.
[2] Pineda JA, Suwal LP, Kelly RB, Bates L, Sloan SW. Characterisation of the Ballina clay. Géotechnique 2016;66(7):556–77.
[3] Kelly RB, Pineda JA, Bates L, Suwal LP, Fitzallen A. Site characterisation for the ballina field testing facility. Geotechnique 2016. 15-P-211.
[4] Vermeer PA, Stolle DFE, Bonnier PG. From the classical theory of secondary compression to modern creep analysis. In: Proc. 9th int. conf. comp. meth. and adv. geomech., Wuhan, China, vol. 4; 1998. p. 2469–78.
[5] Karstunen M, Sivasithamparam N, Brinkgreve RBJ, Bonnier PG. Modelling rate-dependent behaviour of structured clays. In: International. conference on installation effects in geotechnical engineering, 24–27 March 2013, Rotterdam; 2013. p. 43–50.
[6] Sivasithamparam N, Karstunen M, Bonnier P. Modelling creep behaviour of anisotropic soft soils. Comput Geotech 2015;69:46–57.
[7] Sivasithamparam N, Castro J. An anisotropic elastoplastic model for soft clays based on logarithmic contractancy. Int J Numer Anal Meth Geomech 2016;40:596–621.
[8] Das BM. Soil mechanics laboratory manual. New York, USA: Oxford University Press; 2002. p. 99–108.
[9] Lunne T, Robertson PK, Powel JJM. Cone penetration testing in geotechnical practice. London: Blackie Academic & Professional; 1997.
[10] Hansbo S. Consolidation of fine-grained soils by prefabricated drains. In: Proc. 10th ICSMFE, 1981, vol. 3; 1981. p. 677–82.
[11] Liu ZQ, Choi JC, Lacasse S, Nadim F. Uncertainty analyses of time-dependent behaviour of Ballina test embankment. Comput Geotech 2017;93:133–49.